

# Probing the top quark flavour-changing neutral current at a future electron-positron collider

Hoda Hesari<sup>1</sup>, Hamzeh Khanpour<sup>1,2</sup>, Morteza Khatiri Yanehsari<sup>1,3</sup>,  
Mojtaba Mohammadi Najafabadi<sup>1</sup>

<sup>1</sup> *School of Particles and Accelerators, Institute for Research in Fundamental Sciences (IPM) P.O. Box 19395-5531, Tehran, Iran*

<sup>2</sup> *Department of Physics, Mazandaran University of Science and Technology, P.O. Box 48518-78413, Behshahr, Iran*

<sup>3</sup> *Department of Physics, Ferdowsi University of Mashhad, P.O.Box 1436, Mashhad, Iran*

## Abstract

We present a study to examine the sensitivity of a future  $e^-e^+$  collider to the anomalous top flavour-changing neutral current (FCNC) to the gluon. To separate signal from background a multivariate analysis is performed on top-quark pair and background events, where one top quark is considered to follow the dominant Standard Model (SM) decay,  $t \rightarrow Wb$ , and the other top decays through FCNC,  $t \rightarrow qg$ , where  $q$  is a  $u$ - or a  $c$ -quark. The analysis of fully-hadronic FCNC decay of the  $t\bar{t}$  pair is also presented. The 95% confidence level limits on the top-quark anomalous couplings are obtained for different values of the center-of-mass energies and integrated luminosities.

PACS Numbers: 13.66.-a, 14.65.Ha

## 1 Introduction

The top-quark, which is the heaviest known elementary particle up to now, plays a special role in search for new physics beyond the Standard Model (SM) in particular through precise measurement of its couplings with other particles. The large mass of the top quark,  $M_{top} = 173.34 \pm 0.27(stat) \pm 0.71(syst)$  [1], that is close to the scale of electroweak symmetry breaking and its interactions with other particles such as the Higgs boson make it an excellent object to investigate the validity of the SM. The anomalous interactions of the top quark can occur in various flavour-changing neutral current (FCNC) processes like  $t \rightarrow qX$ , where  $X = g, \gamma, Z$  or Higgs. In [2], the anomalous  $tq\gamma$  and  $tqZ$  have been probed at a future electron-positron collider. In the present study, we focus on the top quark FCNC interactions involving the top-quark, a light quark  $q$ , ( $u$ - or  $c$ -quark), and a gluon. In the SM, the FCNC transition of  $t \rightarrow qg$  ( $q = u, c$ ) is forbidden at tree level due to the Glashow-Iliopoulos-Mainai (GIM) mechanism [3] and only

can proceed through the loop corrections. In the SM framework, the loop-level branching ratio for  $t \rightarrow qg$  ( $q = u, c$ ) is of the order of  $10^{-12}$  [4, 5]. Clearly, a lot of data is needed to enable us to observe such a decay process and measure this small branching ratio. Various models beyond the SM could lead to a very large increase in FCNC processes involving the top-quark. Thus, any evidence of such processes will indicate the existence of new physics. In models beyond SM such as MSSM, Technicolor, extra dimensions models higher branching ratios up to  $10^{-3}$  -  $10^{-5}$  are predicted [6, 7, 8] which can be tested by present high energy experiments. There are several phenomenological studies in search for the anomalous  $tqg$  couplings at the Tevatron and LHC and other experiments through different channels [9, 10, 11, 12]. At present the best and up-to-date experimental limits on the  $tqg$  branching fractions come from the direct top production process at the Large Hadron Collider (LHC) by the ATLAS Collaboration,  $Br(t \rightarrow ug) < 3.1 \times 10^{-5}$  and  $Br(t \rightarrow cg) < 1.6 \times 10^{-4}$  at a center-of-mass energy of  $\sqrt{s} = 8$  TeV corresponding to an integrated luminosity of  $\mathcal{L}_{int} = 14.2 \text{ fb}^{-1}$  [13, 14].

It is expected that the future TeV scale linear colliders such as Compact Linear Collider (CLIC) or International Linear Collider (ILC) would complete the LHC probes and even in some processes can improve the measurements and limits. The high luminosity and clean experimental environments of the TeV scale  $e^-e^+$  collider make it an excellent precision machine for the investigation of the top-quark properties. It also provides us an important opportunity for precise measurements of the FCNC couplings in top quark sector [2, 15]. For example, in [2, 15] it has been shown that the branching ratios of the top quark decay into a photon and a Z-boson can be measured up to the order of  $10^{-6}$  at a linear electron-positron collider.

The  $e^-e^+$  collider, CLIC, is designed to operate with the center-of-mass energies of  $\sqrt{s} = 0.5, 1.5$  and  $3$  TeV corresponding to total luminosity of  $L = 2.3, 3.2$  and  $5.9 \times 10^{34} \text{ cm}^{-2} \text{ s}^{-1}$ , respectively [16, 17, 18, 19]. The design of ILC is to work at the center-of-mass energies from  $\sqrt{s} = 0.25$  TeV to  $0.5$  TeV with the option of upgrading to  $1$  TeV. The plan for the ILC instantaneous luminosities is to reach  $10^{33} - 10^{34} \text{ cm}^{-2} \text{ s}^{-1}$  [20, 21]. One of the main differences between the ILC and CLIC is the difference in the luminosity spectrum (LS) of the these machines. The ILC luminosity spectrum has a narrower peak of luminosity. This leads to an increase of the total luminosity and consequently reducing the statistical uncertainty in the measurements.

In this work, we study the sensitivity of a future electron-positron collider (CLIC or ILC) to the anomalous top flavour-changing neutral current (FCNC) to the gluon,  $t - q - g$ . To separate signal from backgrounds, a multivariate technique is used. We consider  $e^-e^+ \rightarrow t\bar{t} \rightarrow qg\ell^+\nu_\ell b(\bar{q}g\ell^-\bar{\nu}_\ell\bar{b})$  (semi-leptonic) and  $e^-e^+ \rightarrow t\bar{t} \rightarrow q\bar{q}gg$  (full-hadronic) separately to search for the anomalous FCNC interactions in  $t - q - g$  vertex. The analysis can also be done in the full hadronic case with one of the top quarks decays into  $t \rightarrow Wb \rightarrow jjj$  and the other top decays through anomalous couplings. Because of the large background contribution the results would be better than the semi-leptonic case therefore we do not perform the analysis for this decay mode. We consider the center-of-mass energies of  $0.5, 1$  and  $1.5$  TeV, and for these energies we analyses two cases, semi-leptonic and fully-hadronic decays of top-quark.

The presented paper is organised as follows: In section 2, we introduce the theoretical formalism which describes the FCNC processes. Section 3 provides a full detailed description of the semi-leptonic channel in search for the  $tqg$  FCNC. The event selection and the methods of event classification into signal- and background-like events using a multivariate analysis are also discussed in this section. Our fully-hadronic analysis is presented in Sec. 4. The results of the investigated FCNC processes, including expected sensitivities on the anomalous couplings and corresponding branching fractions, are given in Sec. 5. Discussions on some detector effects and systematic uncertainties are also presented in Sec. 5. Section 6 contains a summary and conclu-

sions of the analysis.

## 2 Theoretical formalism

In this section, we give a brief overview of the theoretical framework for top FCNC which this analysis is based on. In this work, to describe the FCNC couplings amongst the top quark, a light quark and a gluon ( $tqg$ ) an effective Lagrangian approach is used. The FCNC anomalous interaction in the vertex of  $tqg$  can be written as follows [22, 23, 24, 25, 26]:

$$\mathcal{L}_{eff} = \sum_{q=u,c} \frac{1}{\Lambda} g_s \kappa_{tqg} \bar{t} \sigma^{\mu\nu} T^a \chi q G_{\mu\nu}^a + h.c. \quad (1)$$

where the  $\kappa_{tqg}$ , with  $q = u, c$ , are dimensionless real parameters that presents the strength of the anomalous couplings and strong coupling constant is denoted by  $g_s$ . In Eq.1,  $T^a = \frac{\lambda^a}{2}$  where  $\lambda^a$  are the Gell-Mann matrices,  $\Lambda$  is the new physics scale,  $G_{\mu\nu}^a$  is the gluon field tensor and  $\sigma^{\mu\nu} = \frac{i}{2}[\gamma^\mu, \gamma^\nu]$ . In the effective Lagrangian  $\chi = f_q^L P_L + f_q^R P_R$  with  $P_L(P_R)$  operators perform the left- (right-) handed projection and  $f_q^{(L,R)}$  are chiral parameters normalized to  $|f_q^L|^2 + |f_q^R|^2 = 1$ . In Fig. 1, we show the top pair production cross section times the branching ratios of one top decay anomalously into  $q + g$  and another one decay leptonically (electron and muon) as well as the top pair production cross section times the branching ratios of both tops decay anomalously into  $q + g$ . It is presented for different center-of-mass energies,  $\sqrt{s} = 0.5, 1$  and  $1.5$  TeV versus the anomalous coupling  $\kappa_{tqg}/\Lambda$ . As it can be seen the  $\sigma(e^-e^+ \rightarrow t\bar{t} \rightarrow qg\ell^-\nu\bar{b}(\bar{q}g\ell^+\nu b))(\frac{\kappa_{tqg}}{\Lambda} = 0.02 \text{ TeV}^{-1}) = 22.2 \text{ fb}$  and  $\sigma(e^-e^+ \rightarrow t\bar{t} \rightarrow qg\bar{q}g(\bar{q}gqg))(\frac{\kappa_{tqg}}{\Lambda} = 0.02 \text{ TeV}^{-1}) = 9.6 \text{ fb}$  for the center-of-mass energy of  $0.5 \text{ TeV}$ . In order to calculate the cross section and simulate the events for the analysis, the FCNC effective Lagrangian has been implemented in the FEYNRULES package [27, 28] then the model has been imported to a Universal FeynRules Output (UFO) module [29] and finally inserted to the MADGRAPH 5 [30]. The values of the cross sections are found to be in agreement with COMPHEP package [31, 32].

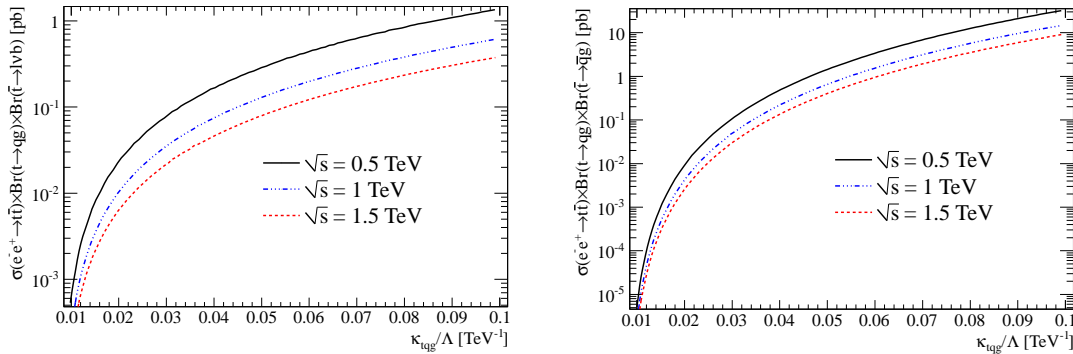


Figure 1: The cross section times branching ratio of one (left) and both (right) of the top quarks decay anomalously into  $q + g$  as a function of the anomalous coupling  $\kappa_{tqg}/\Lambda$  for  $\sqrt{s} = 0.5, 1$  and  $1.5 \text{ TeV}$ .

### 3 Semi-leptonic channel

This section presents the analysis of our signal and the corresponding backgrounds of semi-leptonic channel of  $t\bar{t}$  events at the  $e^-e^+$  collider. In this channel, one of the top-quarks decays through SM decay mode of  $t \rightarrow Wb \rightarrow \ell\nu_\ell b$  ( $\ell = e, \mu$ ) and the other one is considered to decay through FCNC into  $q + g$ , where  $q$  is  $u$  or  $c$  quark. The hadronic final states of W boson have larger background contribution which would not lead to better sensitivity with respect to the semi-leptonic channel. Therefore, the leptonic decay modes of the W-boson that provide cleaner signature is considered. The final state signal topology consists of an energetic lepton, neutrino (appears as missing momentum) and three hadronic jets. One of the jets is originated from a b-quark. The representative Feynman diagram for the signal process is depicted in Fig. 2.

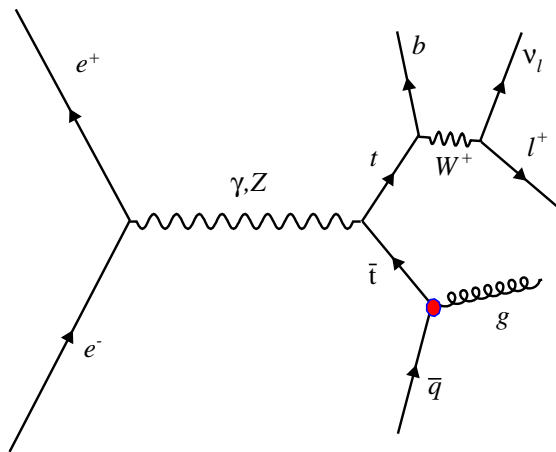


Figure 2: The representative Feynman diagram for the signal process in the semi-leptonic channel.

Based on the expected signature of the signal events, the background topology is therefore given by  $W^\pm jjj \rightarrow \ell^\pm \bar{\nu}_\ell jjj$ . In order to investigate the possibility of separating signal from the background events, we use Monte Carlo (MC) simulation. The MC generation of the signal sample,  $t\bar{t} \rightarrow b\ell\nu_\ell qg$  is done with COMPHEP [31, 32] and the complete set of  $\ell\nu + 3j$  background including the SM process  $t\bar{t} \rightarrow \ell\bar{\nu}_\ell jjj$  are generated using MADGRAPH [30]. The symbol  $j$  represents any jet that originates from quarks and gluon.

To account for the resolution of detectors, we apply energy smearing effects to the final state particles according to the following relations [33, 34]:

$$\frac{\Delta E_{jet}}{E_{jet}} = \frac{40\%}{\sqrt{E_{jet}}} \oplus 2.5\%, \quad \frac{\Delta E_\ell}{E_\ell} = \frac{15\%}{\sqrt{E_\ell}} \oplus 1\% \quad (2)$$

where  $E_{jet}$  and  $E_\ell$  represent the energy of the jets and leptons, respectively. The energies are in GeV and the terms are added in quadrature. The jet energies are smeared according to a Gaussian distribution. We smear the energies of muons similar to the electrons for simplicity. Notice that better resolutions for leptons and jet leads improve the results. We apply the detector acceptance cuts on the transverse momenta of leptons (jets),  $p_T > 20(30)$  GeV, and pseudorapidities,  $|\eta| < 2.5$ . In order to have well-isolated objects, it is required that the distances in  $(\eta, \phi)$  space between each

two objects satisfies  $\Delta R_{ij} = \sqrt{(\eta_i - \eta_j)^2 + (\phi_i - \phi_j)^2} > 0.4$ . It is assumed that the presence of a high- $p_T$  electron or muon plays would be sufficient for triggering the signal events.

Now, the signal events are reconstructed as follows. A full reconstruction of the W boson four-momentum ( $p_W$ ) is needed to be able to reconstruct the semi-leptonic decaying top that is the combination of the reconstructed W and  $b$ -jet,  $M_{Wb-jet}^{rec}$ . It should yield a distribution consistent with the top-quark invariant mass,  $M_{top}$ .

Due to undetected neutrino which leaves no track in the detector, we have difficulties in reconstruction of the W boson. The transverse components of the neutrino momentum ( $p_T^\nu$ ), can be identified by the missing transverse momentum of the events. The longitudinal component of the momentum of the neutrino,  $p_z^\nu$ , can be found by solving the following quadratic equation:

$$p_W^2 = (p_\ell + p_\nu)^2 = M_W^2 \quad (3)$$

which we put a mass constraint on W,  $M_W = 80.4$  GeV. Solving the above quadratic equation allows us to obtain the longitudinal component of the neutrino momentum. This equation has up to two real solutions. In the case of having two real solutions, the one with minimum absolute value is taken. For the events with complex solution only the real part of the solution is considered as the  $z$ -component of the neutrino momentum.

We assume a  $b$ -tagging efficiency of about 60% for  $b$ -jets, 5% for  $c$ -quarks and 1% for lighter quarks to be mis-tagged as  $b$ -quark jets [35, 36]. In order to reconstruct the invariant mass of the semi-leptonic decaying top-quark,  $M_{top}$ , we require a completely reconstructed W boson and a  $b$ -tagged jet. The anomalously decaying top-quark will be reconstructed by combination of two other remaining jets, which are not tagged as  $b$ -jets. The reconstructed invariant masses of both top quarks should have mass closest to the physical top-quark mass,  $M_{top}$ . In some events, there can be more than one  $b$ -tagged jets. To make the correct combination of the jets, the event reconstruction is completed by minimizing a  $\chi_{abc}^2$  defined as:

$$\chi_{abc}^2 = (M_{jajb}^{rec} - M_{top})^2 + (M_{jcW}^{rec} - M_{top})^2 + \Delta R_{jc\ell}^2. \quad (4)$$

where  $M_{jajb}^{rec}$  is the reconstructed mass of the anomalously decaying top quark and  $M_{jcW}^{rec}$  is the reconstructed mass of the top-quark decaying through SM.  $\Delta R_{jc\ell}^2$  is the angular distance between lepton and jets. It is expected that the jet originating from the semi-leptonic top quark decay to be to close to the charged lepton. Various combinations of  $\chi_{abc}$  are made and the one with the minimum  $\chi^2$  is chosen. The minimum value of  $\chi^2$  implies that the reconstructed particles fit the requirement of coming from FCNC or SM top-quark decay. The reconstructed top-quark mass distribution,  $M_{jajb}^{rec}$  and  $M_{Wjc=b-jet}^{rec}$ , for signal and corresponding background at center-of-mass energy of  $\sqrt{s} = 0.5$  TeV are shown in Fig. 3. In Table 1 (left side), we show the number of signal and background events before and after the kinematical cuts for an integrated luminosity of 100 fb $^{-1}$ . In this table, the numbers are presented after including the  $b$ -tagging efficiency.

Certainly, a detailed background study is essential in order to separate the signal from the background events. We use TMVA [37, 38] as a toolkit for multivariate analysis to separate signal from background. Indeed, a multivariate analysis technique is necessary because a single variable doesn't have sufficient discrimination power to separate signal from background events. Among the multivariate analysis techniques are used to separate the signal from the backgrounds boosted decision trees (BDT) is chosen [39, 40, 41]. We choose the variables which have the most possible separation power between the signal from background events for the BDT input. The kinematical variables are selected as input to the BDT are as follow: The reconstructed top quarks masses, the transverse momenta of the  $b$ -jet  $p_T(b)$  and charged lepton  $p_T(\ell)$ , the difference of the azimuthal angle between the reconstructed W boson and the  $b$ -jet  $|\Delta\phi_{W,b-jet}|$ ,

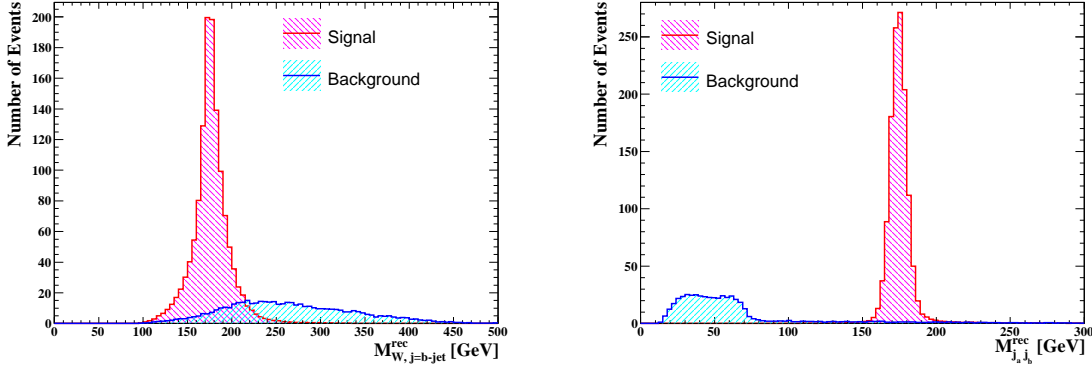


Figure 3: Reconstructed top-quark mass distributions of the W-boson and b-jet  $M_{W,jc=b-jet}^{rec}$  (left), and other two-jet  $M_{j_a j_b}^{rec}$  (right) after the preselection cuts, at  $\sqrt{s} = 0.5$  TeV. The number of events are normalized to  $100 \text{ fb}^{-1}$  integrated luminosity of data and for the signal  $\kappa_{tqg}/\Lambda = 0.02 \text{ TeV}^{-1}$ .

the pseudorapidity distribution of  $b$ -jet  $|\eta_{b-jet}|$ , the invariant mass of the reconstructed W boson  $M_{\ell\nu}^{rec}$ , and finally the angular separation between charged lepton and  $b$ -jet  $\Delta R_{\ell,b-jet}$ . The variable list can be extended and more variables could be given in the BDT input for better discrimination between signal and backgrounds. The kinematic distributions of some used variables which has the most discrimination power are presented in Fig. 4 before applying the acceptance cuts. These distributions are normalized to unity.

These variables are given to the BDT and the multivariate analysis is performed to achieve the best separation between signal and backgrounds and enhance signal significance. The test and training processes are done using a mixture of 50% of signal and 50% of background events. Due to the sensitivity of the BDT classifier to the statistical fluctuation of the training data sample, we use Adaptive Boosting algorithm to increase the performance. In order to avoid overtraining and to improve the quality of the analysis, the BDT built-in options such as Cost Complexity pruning methods are implemented during the training process. The goal is to find the best cuts that enhance the signal and reduce the background. Obtaining best cuts is generally done by finding the maximum value of the statistical significance,  $\frac{n_s}{\sqrt{n_s+n_b}}$ , where  $n_s$  is the number of signal events and  $n_b$  is the number of background event. By choosing the optimum cuts on the BDT output spectrum, we determine the number of selected signal and background events that provide the best signal significance. The results will be discussed in Section 5.

## 4 Fully-hadronic decays of the $t\bar{t}$

In pervious section, we discussed the signal and background where one of the top quarks decays through SM decay mode  $t \rightarrow bW \rightarrow \ell\nu b$  and the other one is considered to decay through FCNC into  $t \rightarrow qg$ . In this section, we consider FCNC decay of both top quarks where the final state consists four-jets at the center of mass energies of  $\sqrt{s} = 0.5, 1$  and  $1.5$  TeV. Specifically, the final state is characterized by the  $t\bar{t}$  events with both top quarks decay into a gluon and a light quark,  $t \rightarrow qg$ .

The representative Feynman diagram for the signal process in the full-hadronic channel is depicted in Fig.5.

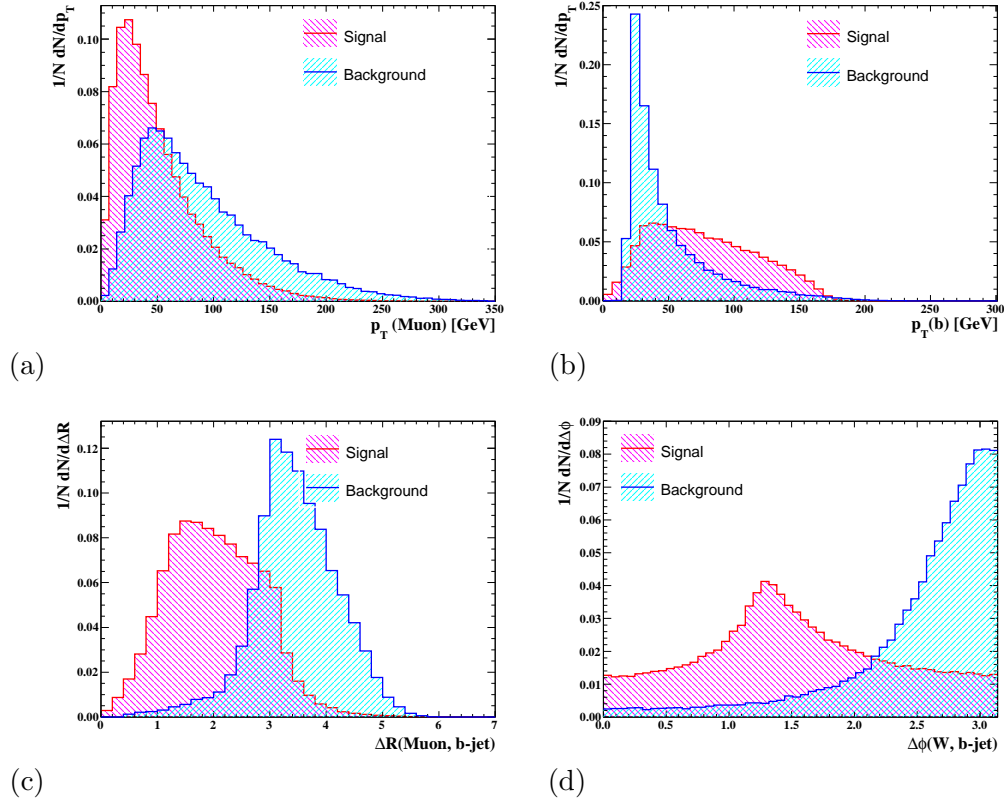


Figure 4: The kinematic distributions of four significance variables used as inputs to BDT in addition to the  $W$  boson and top mass distributions. (a) The transverse momentum of the charged lepton  $p_T(\ell)$  and (b) transverse momentum of the  $b$ -jet  $p_T(b)$ . (c) The angular separation between charged lepton and  $b$ -jet  $\Delta R_{\ell, b\text{-jet}}$  and (d) the difference of the azimuthal angle between the reconstructed  $W$  boson and the  $b$ -jet  $|\Delta\phi_{W, b\text{-jet}}|$ .

It is worth mentioning that hadron colliders may not be a good area to study this fully hadronic process due to the extremely large QCD background contributions. The linear electron-positron colliders such as CLIC or ILC have a clean environment, consequently these fully hadronic final states can be probed at the CLIC or ILC easier than the hadron colliders.

The method of the channel is similar to semi-leptonic one that presented in the previous section. The MC generation of the signal sample is generated with COMPHEP and the complete set of four-jets background is done using MADGRAPH 5.

The same as the semi-leptonic case, to account for the resolution of the detectors a Gaussian energy smearing is performed on the final states jets. The jets are required to have transverse momenta greater than 30 GeV within the pseudorapidity acceptance range of  $|\eta| < 2.5$ . It is also required that  $\Delta R_{ij} = \sqrt{(\eta_i - \eta_j)^2 + (\phi_i - \phi_j)^2} > 0.4$ . The number of events before and after the kinematical cuts are shown in the right side of Table 1 for an integrated luminosity of  $100 \text{ fb}^{-1}$ . The reconstructed top-quark mass distributions for signal and the corresponding background at center-of-mass energy of  $\sqrt{s} = 0.5 \text{ TeV}$  are shown in Fig. 6 for an integrated luminosity of  $100 \text{ fb}^{-1}$ . The number of signal events in these figures have been multiplied by a factor of 10.

Again we use the Boosted Decision Tree (BDT) classifier of the TMVA package for discrimi-

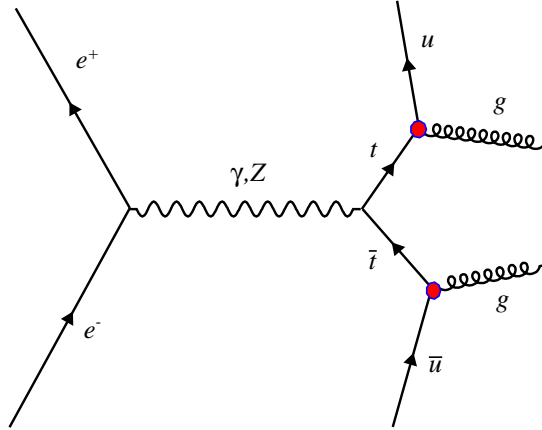


Figure 5: The representative Feynman diagram for the signal process in the hadronic channel.

nating signal from background events. For the BDT algorithm, the simulated events of the signal and background are split up in two similar samples for the training and test processes.

The input kinematical variables to the BDT are the reconstructed top-quark masses  $M_{top}^{rec}$ , the transverse momentum of the highest  $P_T$  jet, the corresponding pseudorapidity distribution  $|\eta_j|$  of the highest  $P_T$  jet, the angular separation  $\Delta R_{j_a j_b}$  between the two jets, and the scalar transverse energy,  $H_T$ . The opening angles  $\Delta\phi_{j_a j_b}$  between the directions of the final state jets is correlated with the mentioned variables so we neglected them. For the fully hadronic top-quark reconstruction, we take the pair of jets which have an invariant mass closest to the nominal top-quark mass as well as having smaller angular distance  $\Delta R_{j_a j_b}$ . In the analysis, an angular resolution of around 100 mrad is assumed due to the expected high granularity design of the calorimeters of the future electron-positron collider [42].

In summary, in this section we concentrated on the channel of top pair production which both top quarks decay anomalously into two jets. After a rough detector simulation and applying the acceptance cuts, optimum kinematical variables are found and given to the BDT for discriminating between signal and backgrounds. In the next section, the limit on the branching fractions are given.

Table 1: The number of events before and after the kinematical cuts for signal and background at a center-of-mass energy of 0.5 TeV and with  $100 \text{ fb}^{-1}$  integrated luminosity of data for semileptonic and full hadronic (both top decay anomalously). The b-tagging efficiencies have been included and for the signal we have set  $\kappa_{tqg}/\Lambda = 0.02 \text{ TeV}^{-1}$ .

Decay mode	Semi-leptonic		Full-hadronic	
	Before cuts	After cuts	Before cuts	After cuts
Signal	2146.5	1297.4	480.0	354.0
Background	1743.2	500.0	58905.1	29211.3



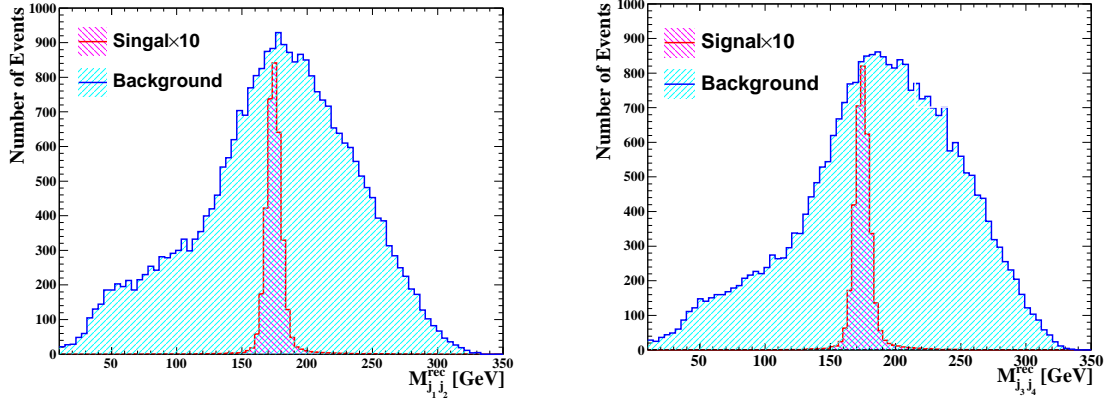


Figure 6: Reconstructed top-quark mass distributions for the anomalous decay of both top quarks into a light-quark and a gluon at  $\sqrt{s} = 0.5$  TeV. The distributions are normalized to  $100 \text{ fb}^{-1}$  integrated luminosity of data and for the signal  $\kappa_{tqg}/\Lambda = 0.02 \text{ TeV}^{-1}$ . The number of signal events are multiplied by a factor 10.

## 5 Results

With assuming of observation no signal events after performing the experiment or in another words, if the number of observed events are equal to the number of expected background events, we proceed to set 95% C.L. upper limit on the signal cross section. Limits on the cross section of signal is calculated with a CLs approach [43]. The RooStats [44] program is used for statistical data analysis for the numerical evaluation of the CLs limits. The program returns the 95% C.L. upper limit on the signal cross section times branching ratios of the top quarks decays.

The sensitivity of the branching fractions as a function of the integrated luminosity for the future electron-positron collider at different center-of-mass energies are shown in Fig. 7 and Fig. 8 for the semi-leptonic and fully-hadronic analyses, respectively. As it can be seen from the figure, higher integrated luminosities lead to better bounds on the branching ratio up to around  $500 \text{ fb}^{-1}$ . The limits at the center of mass energy of 0.5 TeV is better than the ones at 1 and 1.5 TeV that is because of the larger cross sections at smaller energies. Comparing the semi-leptonic channel with the full-hadronic one, better sensitivity is achieved in the semi-leptonic channel. It is again due to the fact that in the full-hadronic channel statistics is poor with respect to the semi-leptonic one. The upper limits on the  $Br(t \rightarrow qg)$  at 95% C.L. with  $500 \text{ fb}^{-1}$  are 0.00117 and 0.0236 for the semi-leptonic and full-hadronic channels, respectively. It is interesting to mention here that the dependence of the expected upper limit on the integrated luminosity becomes weaker at luminosities larger than  $500 \text{ fb}^{-1}$ .

Now, the sensitivity of the results on the detector performance is discussed. In this analysis, almost all sub-detectors are involved to identify and reconstruct leptons, jets, b-jets and missing energy. Precise reconstruction of secondary vertex for an efficient b-tagging is necessary in this analysis to suppress the backgrounds and obtain a pure signal sample. The variation of b-tagging efficiency in this analysis by 10% leads to approximately 4% change in the expected upper limit on the branching ratio. The resolution in measurement of the jet and lepton energies are less important than b-jet identification. Varying the resolution in jet and lepton energy measurement by 10% and 5% (Eq.2) leads to change the upper limit on the branching fraction by less than 1%.

In this analysis, we have calculated the cross section for the energy at the vertex of electron-positron. Therefore, further effects such as the initial state radiation (ISR) and the luminosity spectrum (LS) of the collider need to be considered. Both the initial state radiation and the luminosity spectrum lead to reduce the cross section. We calculate the effect of ISR to the cross section at the center-of-mass energy of 500 GeV. The signal cross section decreases by a round 2% which leads to loose the expected upper limit on the branching ratio from 0.00117 to 0.00118 with  $500 \text{ fb}^{-1}$ .

To have a more realistic analysis, the effects of the systematic uncertainties should be estimated. The uncertainties can arise from jet energy scale, lepton energy, lepton reconstruction identification efficiencies, b-tagging efficiency and uncertainties on the masses of the top quark and W-boson. We vary the b-tagging efficiency by  $\pm 5\%$ . This leads to change the expected upper limit by 1.5%. To estimate the uncertainty from jet energy scale, we vary the energy of each jet by 2% and recalculate the limit. It results to a change of 0.5% on the expected upper limit. The uncertainties on the top quark and W boson masses are calculated as follows: We generate new signal samples with varied top mass ( $\pm 1 \text{ GeV}$ ) and W boson mass ( $\pm 50 \text{ MeV}$ ) and re-do the analysis. This leads to a change of 0.05% on the expected upper limit on the branching fraction of  $t \rightarrow qg$ .

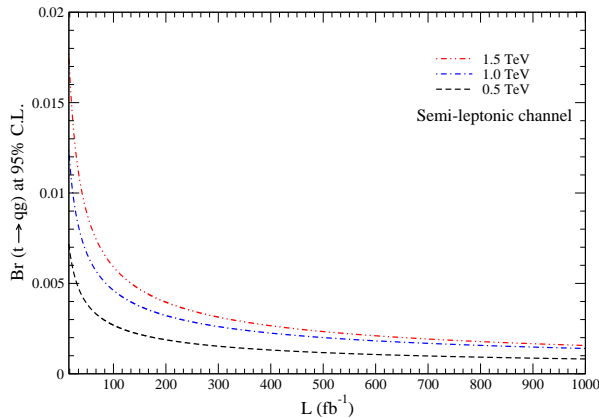


Figure 7: The 95% C.L. upper limits for  $Br(t \rightarrow qg)$  as a function of integrated luminosity for  $\sqrt{s} = 0.5, 1$  and  $1.5 \text{ TeV}$  for the semi-leptonic analysis.

### 5.1 Comparison with the LHC Results

So far, we have examined the future  $e^-e^+$  collider potential to probe the anomalous  $tqg$  in the decay of the top quark in top pair production. At hadron colliders, the anomalous  $tqg$  couplings can be probed either in top production or top decay. The best limits have been obtained in the production processes. There are different production channels to search for the anomalous  $tqg$ : (1) direct top quark production ( $2 \rightarrow 1$  process), (2) Single top quark production ( $2 \rightarrow 2$ ), (3) double top pair ( $t\bar{t}, t\bar{t}$ ) production and (4) top plus vector boson production ( $tV$ ) [45]. Currently, the strongest experimental limits on the  $tqg$  branching fractions come from the direct top production ( $2 \rightarrow 1$  process) at the LHC by the ATLAS Collaboration,  $Br(t \rightarrow ug) < 3.1 \times 10^{-5}$  and  $Br(t \rightarrow cg) < 1.6 \times 10^{-4}$  at a center-of-mass energy of  $\sqrt{s} = 8 \text{ TeV}$  corresponding to an integrated luminosity of  $\mathcal{L}_{int} = 14.2 \text{ fb}^{-1}$  [13].

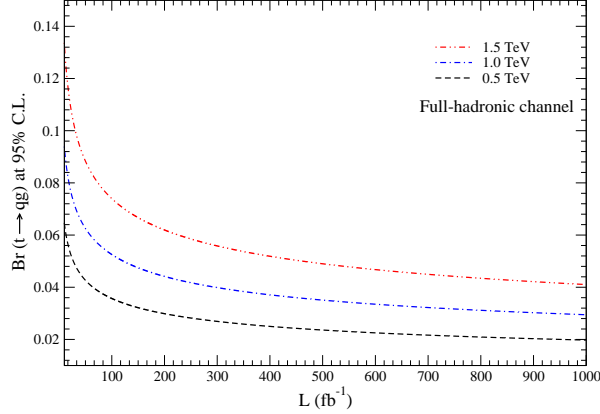


Figure 8: The 95% C.L. upper limits for  $Br(t \rightarrow qq)$  as a function of integrated luminosity for  $\sqrt{s} = 0.5, 1$  and  $1.5$  TeV for the fully-hadronic analysis.

In [46], the anomalous  $tqg$  couplings have been probed in top decay at the Tevatron. The obtained upper limit on the branching ratio is  $5(2.7) \times 10^{-3}$  with  $10$  ( $30$ )  $\text{fb}^{-1}$  of data. These limits are weaker in comparison with the limits that can be obtained from the production processes.

The future LHC bounds at  $14$  TeV center-of-energy using  $100 \text{ fb}^{-1}$  of data using various processes are compared with the ones obtained in this work are compared in Table 2. As it can be seen, among the all processes the  $2 \rightarrow 1$  process provides the strongest limit ( $10^{-6}$ ). The limits that we have obtained in this study for  $e^-e^+$  collider are comparable with the ones that come out of the same-sign top ( $t\bar{t}, t\bar{t}$ ) production at the LHC and the ones from top decays in top pair events at the Tevatron.

Table 2: The 95% C.L. upper limit on the  $Br(t \rightarrow qq)$  with the LHC ( $8, 14$  TeV) and  $e^-e^+$  ( $0.5$  TeV) based on  $100 \text{ fb}^{-1}$  integrated luminosity of data. The results of LHC8 is corresponding to  $14.2 \text{ fb}^{-1}$ .

Collider	LHC8 ( $14.2 \text{ fb}^{-1}$ )	LHC14 ( $100 \text{ fb}^{-1}$ )					$e^-e^+$ ( $100 \text{ fb}^{-1}$ )
Process	$2 \rightarrow 1$	$2 \rightarrow 1$	$2 \rightarrow 2$	$tV$	$t\bar{t}, t\bar{t}$		$t\bar{t}$
Upper limit	$3.1 \times 10^{-5}$	$10^{-6}$	$10^{-5}$	$10^{-5}$	$10^{-3}$		$10^{-3}$

## 6 Summary and conclusions

In this paper, we have studied the signals of top quark flavor-changing neutral current in the vertex of  $tqg$ , where  $q = u$  and  $c$ , at a future electron-positron collider. This study has been done by looking at the top pair production and at three different center of mass energies of  $0.5, 1$  and  $1.5$  TeV in the top quarks decays. We have investigated two possible cases: first one is the case that one top quark decays anomalously to  $q + g$  and another one follows SM decay to a W boson and a b-quark and W boson decays leptonically ( $e^-e^+ \rightarrow t\bar{t} \rightarrow qq\ell^+\nu_\ell b$ ). Second is that both top quarks decay anomalously through FCNC decay mode ( $e^-e^+ \rightarrow t\bar{t} \rightarrow q\bar{q}gg$ ). Using the Boosted Decision Tree (BDT) technique, we discriminate between signal and backgrounds. Then the CLs approach has been utilized to set upper limits on the branching ratio. The 95% C.L. upper limit

on the branching ratio using  $500 \text{ fb}^{-1}$  of data at the center of mass energy of 0.5 TeV is 0.00117 (0.0236) in semi-leptonic (full-hadronic) channel. It is shown that the limit is improved with the integrated luminosity up to around  $500 \text{ fb}^{-1}$  and the dependence of the expected upper limit on the integrated luminosity becomes weaker at luminosities larger than  $500 \text{ fb}^{-1}$ .

We have found that sensitivity to the anomalous couplings decreases with increasing the center of energy of the collisions simply due to the decrease in the signal cross section with growing the center of mass energy. The expected bounds are comparable with the ones that is obtained from the double top production at the LHC ( $t\bar{t}, t\bar{t}$ ) and from the anomalous top decay in top pair events at Tevatron.

## Acknowledgments

We are grateful to R. Goldouzian for valuable discussions. We acknowledge financial support of the School of Particles and Accelerators, Institute for Research in Fundamental Sciences (IPM).

## Conflict of Interests

The authors declare that there is no conflict of interests regarding the publication of this paper.

## References

- [1] [ATLAS and CDF and CMS and D0 Collaborations], arXiv:1403.4427 [hep-ex].
- [2] J. A. Aguilar-Saavedra, Phys. Lett. B **502**, 115 (2001) [hep-ph/0012305].
- [3] S. L. Glashow, J. Iliopoulos and L. Maiani, Phys. Rev. D **2**, 1285 (1970).
- [4] G. Eilam, J. L. Hewett, and A. Soni, Phys. Rev. D **44**, 1473 (1991).
- [5] B. Mele, S. Petrarca and A. Soddu, Phys. Lett. B **435**, 401 (1998) [hep-ph/9805498].
- [6] S. Bejar, J. Guasch, D. Lopez-Val and J. Sola, Phys. Lett. B **668**, 364 (2008) [arXiv:0805.0973 [hep-ph]].
- [7] J. Cao, Z. Heng, L. Wu and J. M. Yang, Phys. Rev. D **79**, 054003 (2009) [arXiv:0812.1698 [hep-ph]]; R. Guedes, R. Santos and M. Won, arXiv:1308.4723 [hep-ph].
- [8] G. A. Gonzalez-Sprinberg and R. Martinez, hep-ph/0605335; R. Coimbra, A. Onofre, R. Santos and M. Won, Eur. Phys. J. C **72**, 2222 (2012) [arXiv:1207.7026 [hep-ph]].
- [9] J. Gao, C. S. Li, L. L. Yang and H. Zhang, Phys. Rev. Lett. **107**, 092002 (2011) [arXiv:1104.4945 [hep-ph]].
- [10] J. -L. Agram, J. Andrea, E. Conte, B. Fuks, D. Gel and P. Lansonneur, Phys. Lett. B **725**, 123 (2013) [arXiv:1304.5551 [hep-ph]].
- [11] S. Khatibi and M. M. Najafabadi, Phys. Rev. D **89**, 054011 (2014) [arXiv:1402.3073 [hep-ph]].
- [12] S. M. Etesami and M. Mohammadi Najafabadi, Phys. Rev. D **81**, 117502 (2010) [arXiv:1006.1717 [hep-ph]].

- [13] The ATLAS collaboration, ATLAS-CONF-2013-063.
- [14] E. Yazgan [ for the ATLAS and CDF and CMS and D0 Collaborations], arXiv:1312.5435 [hep-ex].
- [15] J. A. Aguilar-Saavedra and T. Riemann, In \*2nd ECFA/DESY Study 1998-2001\* 2428-2450 [hep-ph/0102197].
- [16] P. Lebrun, L. Linssen, A. Lucaci-Timoce, D. Schulte, F. Simon, S. Stapnes, N. Toge and H. Weerts *et al.*, arXiv:1209.2543 [physics.ins-det].
- [17] "Miyamoto, Akiya and Stanitzki, Marcel and Weerts, Harry and Linssen, Lucie", Report", [arXiv:1202.5940], CERN-2012-003. ANL-HEP-TR-12-01. DESY-12-008. KEK-Report-2011-7,
- [18] J. E. Brau, R. M. Godbole, F. R. L. Diberder, M. A. Thomson, H. Weerts, G. Weiglein, J. D. Wells and H. Yamamoto, arXiv:1210.0202 [hep-ex].
- [19] MAicheler, MAicheler, PBurrows, MDraper, TGarvey, PLebrun, KPeach and NPhinney *et al.*, CERN-2012-007.
- [20] H. Baer, T. Barklow, K. Fujii, Y. Gao, A. Hoang, S. Kanemura, J. List and H. E. Logan *et al.*, arXiv:1306.6352 [hep-ph].
- [21] T. Behnke, J. E. Brau, B. Foster, J. Fuster, M. Harrison, J. M. Paterson, M. Peskin and M. Stanitzki *et al.*, arXiv:1306.6327 [physics.acc-ph].
- [22] W. Buchmuller and D. Wyler, Nucl. Phys. B **268**, 621 (1986).
- [23] E. Malkawi and T. M. P. Tait, Phys. Rev. D **54**, 5758 (1996) [hep-ph/9511337].
- [24] M. Hosch, K. Whisnant and B. L. Young, Phys. Rev. D **56**, 5725 (1997) [hep-ph/9703450].
- [25] J. A. Aguilar-Saavedra, Nucl. Phys. B **812**, 181 (2009) [arXiv:0811.3842 [hep-ph]].
- [26] J. Gao, C. S. Li, L. L. Yang and H. Zhang, Phys. Rev. Lett. **107**, 092002 (2011) [arXiv:1104.4945 [hep-ph]].
- [27] N. D. Christensen and C. Duhr, Comput. Phys. Commun. **180**, 1614 (2009) [arXiv:0806.4194 [hep-ph]].
- [28] C. Duhr and B. Fuks, Comput. Phys. Commun. **182**, 2404 (2011) [arXiv:1102.4191 [hep-ph]].
- [29] C. Degrande, C. Duhr, B. Fuks, D. Grellscheid, O. Mattelaer and T. Reiter, Comput. Phys. Commun. **183**, 1201 (2012) [arXiv:1108.2040 [hep-ph]].
- [30] J. Alwall, M. Herquet, F. Maltoni, O. Mattelaer and T. Stelzer, JHEP **1106**, 128 (2011) [arXiv:1106.0522 [hep-ph]].
- [31] E. Boos, V. Bunichev, M. Dubinin, L. Dudko, V. Edneral, V. Ilyin, A. Kryukov and V. Savrin *et al.*, PoS ACAT **08**, 008 (2008) [arXiv:0901.4757 [hep-ph]].
- [32] E. Boos *et al.* [CompHEP Collaboration], Nucl. Instrum. Meth. A **534**, 250 (2004) [hep-ph/0403113].

- [33] L. Linssen, A. Miyamoto, M. Stanitzki, H. Weerts, arXiv:1202.5940 [physics.ins-det].
- [34] J. Brau *et al.* [ILC Collaboration], arXiv:0712.1950 [physics.acc-ph].
- [35] H. Baer, T. Barklow, K. Fujii, Y. Gao, A. Hoang, S. Kanemura, J. List and H. E. Logan *et al.*, arXiv:1306.6352 [hep-ph].
- [36] H. Abramowicz *et al.* [CLIC Detector and Physics Study Collaboration], arXiv:1307.5288 [hep-ex].
- [37] J. Therhaag, PoS ICHEP **2010**, 510 (2010).
- [38] A. Hocker *et al.*, arXiv:physics/0703039.
- [39] B. P. Roe, H. -J. Yang, J. Zhu, Y. Liu, I. Stancu and G. McGregor, Nucl. Instrum. Meth. A **543**, 577 (2005) [physics/0408124].
- [40] H. -J. Yang, B. P. Roe and J. Zhu, Nucl. Instrum. Meth. A **555**, 370 (2005) [physics/0508045].
- [41] H. -J. Yang, B. P. Roe and J. Zhu, Nucl. Instrum. Meth. A **574**, 342 (2007).
- [42] Roman Poschl, Journal of Physics: Conference Series 293, 012069 (2011).
- [43] A. L. Read, Modified frequentist analysis of search results (the CL(s) method), in Workshop on Confidence Limits, p. 81. Geneva, Switzerland, 2000.
- [44] L. Moneta *et al.*, The RooStats Project, ACAT2010 Conference Proceedings, (2010) arXiv:1009.1003.
- [45] M. Beneke, I. Efthymiopoulos, M. L. Mangano, J. Womersley, A. Ahmadov, G. Azuelos, U. Baur and A. Belyaev *et al.*, In \*Geneva 1999, Standard model physics (and more) at the LHC\* 419-529 [hep-ph/0003033].
- [46] T. Han, K. Whisnant, B. L. Young and X. Zhang, Phys. Lett. B **385**, 311 (1996) [hep-ph/9606231].